

Characterization of Ionic Currents in Human Neural Stem Cells

Chae Gil Lim^{1,2}, Sung-Soo Kim³, Haeyoung Suh-Kim³, Young-Don Lee³, and Seung Cheol Ahn¹

¹Department of Physiology, College of Medicine, Dankook University, Cheonan 330-714, ²Department of Physical Therapy, Gachon University of Medicine and Science, Incheon 406-799, ³Department of Anatomy, Ajou University School of Medicine, Suwon 443-749, Korea

The profile of membrane currents was investigated in differentiated neuronal cells derived from human neural stem cells (hNSCs) that were obtained from aborted fetal cortex. Whole-cell voltage clamp recording revealed at least 4 different currents: a tetrodotoxin (TTX)-sensitive Na⁺ current, a hyperpolarization-activated inward current, and A-type and delayed rectifier-type K⁺ outward currents. Both types of K⁺ outward currents were blocked by either 5 mM tetraethylammonium (TEA) or 5 mM 4-aminopyridine (4-AP). The hyperpolarization-activated current resembled the classical K⁺ inward current in that it exhibited a voltage-dependent block in the presence of external Ba²⁺ (30 μM) or Cs⁺ (3 μM). However, the reversal potentials did not match well with the predicted K⁺ equilibrium potentials, suggesting that it was not a classical K⁺ inward rectifier current. The other Na⁺ inward current resembled the classical Na⁺ current observed in pharmacological studies. The expression of these channels may contribute to generation and repolarization of action potential and might be regarded as functional markers for hNSCs-derived neurons.

Key Words: Human neural stem cells, TTX-sensitive Na⁺ current, A-type, delayed rectifier, hyperpolarization-activated inward current

INTRODUCTION

Neural stem cells (NSCs) are primordial, uncommitted cells with the ability to proliferate and differentiate into cells of all neuronal lineages (Weiss et al, 1996; Flax et al, 1998) and many investigators have developed neural stem cells of adult, fetal and embryonic origins (Carpenter et al, 2001; Westerlund et al, 2003; Ilancheran et al, 2007) for their potential therapeutic use in neurological disorders. In the development of neural stem cells, the differentiation of neural stem cells into true functional neurons has been a major focus of interest and many researchers have studied the electrophysiological properties of differentiated neurons because the immunological characterization of neuronal markers does not necessarily reflect neuronal differentiation (Balasubramanian et al, 2004).

The most thorough study concerning electrophysiological properties of differentiated human neural precursor cells might be that of Piper et al. who demonstrated two different K⁺ outward currents (A-type and delayed rectifier), an inward rectifier K⁺ current and two different Na⁺ inward currents (TTX-sensitive and -insensitive). They also observed an inward Ca²⁺ current but they did not show the raw data (Piper et al, 2000). Among the currents reported by Piper et al., the K⁺ outward currents and the Na⁺ inward currents have also been investigated in many other studies using hNSCs from different sources (Cho et al, 2002; Sun et al, 2005; Johnson et al, 2007). This is due to the fact

that these currents are regarded as markers for functionally differentiated neurons in terms of generation and repolarization of action potential.

To date, many investigators have reported the ionic channel expression patterns in differentiated neurons from different sources such as spinal cord (Akesson et al, 2007), adult brain (Moe et al, 2005b), umbilical cord blood (Buzanska, et al, 2006), bone marrow (Mareschi et al, 2006), etc. However, ionic channel expression patterns of differentiated neurons from non-immortalized hNSCs derived from human fetal brain have rarely been reported. In the present study, therefore, we characterized the ionic currents of differentiated neurons derived from primary dissociated cell cultures of fetal cortical brain (14 weeks of gestation).

METHODS

Neural stem cell culture

Cortical tissue was obtained from a 14-week-old aborted human fetus at Ajou University Medical Center according to the guidelines approved by the Institutional Review Board of Ajou University Medical Center (Suwon, Korea). In short, cortical tissue was microdissected and then mechanically dissociated to form a single cell suspension. Cells were maintained at 37°C in a humidified atmosphere with 5% CO₂, plated on fibronectin-coated glass coverslips and incubated with expansion medium. Expansion medium (DMEM:F12, 1 : 1; Gibco, Grand Island, NY, USA; L-glutamine, 2.92 g/100 ml; HEPES, 23.8 mg/100 ml; NaHCO₃, 7.5%; glucose, 0.6%; and heparin, 2%) contained B27-supplement (1%; Gibco), human leukemia inhibitory factor (10

Corresponding to: Seung Cheol Ahn, Department of Physiology, College of Medicine, Dankook University, San 29, Anseo-dong, Cheonan 330-714, Korea. (Tel) 82-41-550-3852, (E-mail) ansil67@dku.edu

ng/ml; Sigma-Aldrich), epidermal growth factor (EGF, 20 ng/ml, R&D Systems, Minneapolis, MN USA), and basic fibroblast growth factor (bFGF, 20 ng/ml, R&D Systems, Minneapolis, MN USA). After 3 days, half of the medium was replaced with neural differentiation medium (both bFGF and EGF were omitted from expansion medium). Over the next 9 days, medium was replaced with fresh neural differentiation medium every 3 days, and the cells were subjected to immunocytochemical and electrophysiological analyses.

Immunostaining

The cells were fixed with a 4% buffered paraformaldehyde solution for 10 min at room temperature. The fixed cells were washed three times with PBS and incubated with 10% normal goat serum in PBS for 1 hour. After sufficient washing, the cells were incubated overnight with primary antibodies against mouse β -tubulin III (Tuj-1; 1 : 200, Covance, Richmond, CA, USA), and mouse glial fibrillary acidic protein (GFAP, Sigma, St. Louis, MO, USA) at 4°C. Following several washes with PBS/0.1% Triton X-100, cells were incubated in Alexa Fluor 568-conjugated anti-mouse IgG (1 : 500, Molecular Probes, Eugene, OR, USA) antibody for 1 hour in a dark chamber. For visualizing cellular nuclei, cells were counterstained with bis-benzamide (Molecular Probes). Fluorescent images were acquired with a Zeiss Axiophot microscope (Zeiss, Jena, Germany). Through this immunostaining procedure, we identified the morphology of Tuj-1-positive cells (neural differentiated cells) and used these cells for electrophysiological analysis (Fig. 1).

Electrophysiology

Neural differentiated cells were placed in a recording chamber on the stage of an inverted microscope (Diaphot 300, Nikon, Japan), and membrane currents were recorded using the whole-cell voltage clamp technique. Patch micro-

pipettes having a resistance of 3~5M Ω were pulled by a glass puller (glass microelectrode puller PP-83, Narishige, Japan) from borosilicate glass capillaries (external diameter 1.5 mm, internal diameter 1.17 mm, Harvard, USA) and fire-polished using a microforge (MF-830, Narishige, Japan). The pipette solution contained (in mM) 145 CsCl, 100 aspartic acid, 2 MgCl₂, 3 Na₂ATP, 10 EGTA, 10 HEPES, and 10 TEA (tetraethylammonium) (290~295 mOsm) for the Na⁺ current measurement, and 155 KCl, 100 aspartic acid, 2 MgCl₂, 7 Na₂ATP, 10 EGTA, 20 HEPES, 10 phosphocreatine (disodium salt) (250~260 mOsm) for measurements of the outward K⁺ current and the hyperpolarization activated current. The pH was adjusted to 7.2 with KOH or CsOH. The bath solution contained (in mM) 147 NaCl, 5 KCl, 10 HEPES, 1.5 CaCl₂, 1 MgCl₂, and 5 glucose (285~290 mOsm) for the Na⁺ current, and 147 NMGCl, 2.5 KCl, 10 HEPES, 1.5 CaCl₂, 1 MgCl₂, and 5 glucose (285~290 mOsm) for measurements of the hyperpolarization activated current and the outward K⁺ current. All chemicals were purchased from Sigma unless otherwise indicated. Data were filtered at 5 kHz (Axon Instruments, USA), digitized at 10 kHz (Digidata1200B, Axon Instruments, USA) and stored on a computer using pClamp 6.0 (Axon Instruments, USA). Analysis of electrophysiological data and statistical tests were performed with clampfit 6.0 (Axon Instruments, USA), and Origin 7.0 (OriginLab corporation). Data are expressed throughout the text as mean \pm standard error of the mean.

RESULTS

Voltage dependent Na⁺ current

With 147 mM NaCl in the bath and 145 mM CsCl and 10 mM TEA in the pipette, membrane depolarization from -90 mV to +40 mV with 10 mV increments elicited inward currents. The peak amplitude observed at -10 mV was -455 \pm

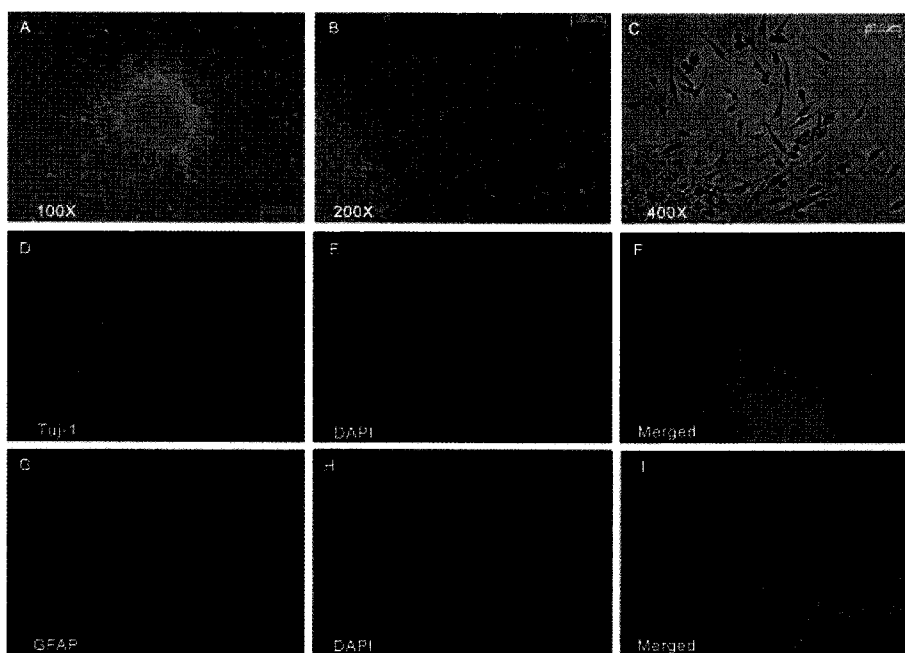


Fig. 1. Immunocytochemistry of differentiated human neural stem cells. Cultured hNSCs were differentiated into neural lineage cells by removing the growth factors from the culture medium. 9 days after neural induction, the cells were immunostained with (D~F) anti- β -tubulin III antibody (Tuj-1), and (G~I) anti-GFAP antibody. Immunostained cells were counterstained with DAPI. Phase contrast images of differentiated hNSCs at 100X, 200X, and 400X magnification are shown in (A~C).

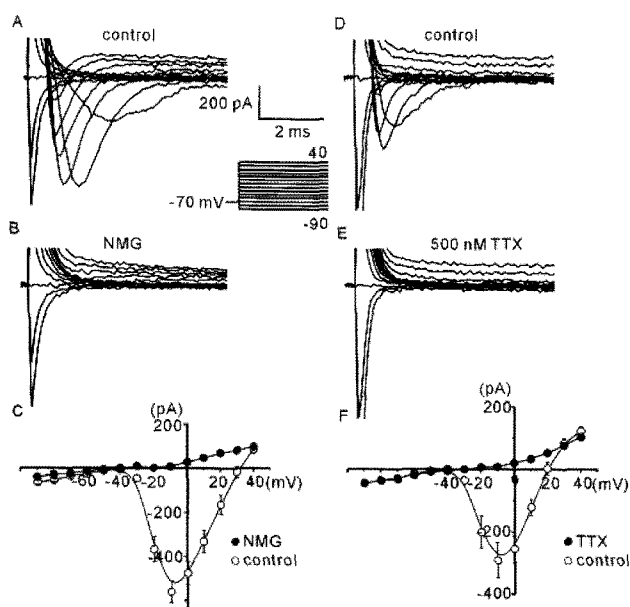


Fig. 2. Voltage-dependent Na^+ current in hNSCs. Membrane depolarization from -90 to 40 mV evoked inward currents (A), which were not observed when external Na^+ was replaced with an equimolar concentration of NMG (B). The I - V relationships of (A) and (B) are shown in (C). Inward currents elicited by the same protocol are blocked completely by 500 nM TTX (D, E). The I - V relationships of (D) and (E) are shown in (F). Hollow circles indicate the amplitudes of peak inward currents of given commanding potentials in the control, and filled circles indicate the current amplitudes remaining after NMG substitution (C) or TTX application (F).

47.95 pA ($n=13$). The inward current was sensitive to 500 nM TTX ($n=7$, Fig. 2D, 2E, 2F) and was reversibly abolished by the substitution of external Na^+ with an equimolar concentration of NMGCl ($n=9$, Fig. 2A, 2B, 2C). The presence or absence of nifedipine (2 μM), a known Ca^{2+} channel blocker, in the bath did not affect the inward currents (data not shown). The reversal potential was dependent on the external concentration of Na^+ ($[\text{Na}^+]_{\text{ext}}$). Upon increasing $[\text{Na}^+]_{\text{ext}}$ from 112.5 mM to 147 mM, the reversal potential shifted from 21.1 ± 1.3 mV to 28.1 ± 0.8 mV ($n=7$). A plot of the reversal potential as a function of $[\text{Na}^+]_{\text{ext}}$ agreed well with the predicted Nernstian relation for a Na^+ -selective conductance: a fit to the data points yielded a slope of 59.9 ± 11.0 mV per $\log[\text{Na}^+]_{\text{ext}}$, whereas the slope of the Nernst equation for a perfectly Na^+ -selective conductance at 25°C was 59.16 mV per $\log[\text{Na}^+]_{\text{ext}}$. The $[\text{Na}^+]_{\text{ext}}$ -dependent change in the reversal potential, TTX-sensitivity and abolishment of inward current by NMGCl replacement indicated that this inward current was a voltage-dependent Na^+ current.

Voltage dependent K^+ outward currents

With 147 mM NMGCl in the bath and 155 mM K^+ in the pipette, membrane depolarization from -90 mV to $+40$ mV with 10 mV increments elicited outward currents that could be divided into two components according to the activation kinetics: fast activating (A-type) and delayed sustained (delayed rectifier type) currents. The A-type current, reaching a peak within 5 ms, was observed in 21 out of 36 cells tested, whereas the delayed rectifier-type current

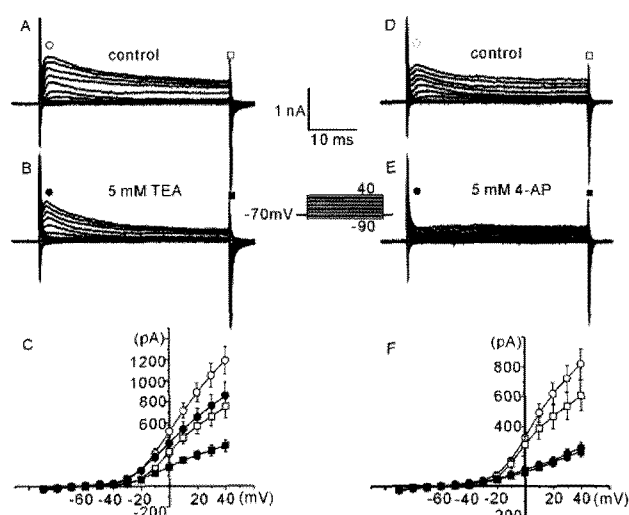


Fig. 3. Voltage-dependent K^+ currents in hNSCs. Depolarizing pulses from -90 to 40 mV elicited outward K^+ currents (A, B, D, E). The symbols above the currents traces indicate the measuring points. Hollow symbols are used in the control current traces, and filled symbols are used in the current traces remaining after the drug applications. I - V relationships before and after the drug applications are shown in (C, F). Hollow circles and squares in (C, F) indicate A-type and delayed rectifier type current amplitudes of each commanding potentials before drug application, while the filled symbols in (C, F) indicate amplitudes of A-type and delayed rectifier type currents after drug application.

was observed in all the cells tested ($n=36$). Pharmacologically, the A-type current was more sensitive to 4-aminopyridine (4-AP) than TEA. Five mM 4-AP reduced the peak A-type current recorded at 40 mV to $31 \pm 1.8\%$ of the control ($n=10$, Fig. 3D, 3E, 3F), while 5 mM TEA reduced the A-type current only to $72.2 \pm 4.5\%$ of the control ($n=11$, Fig. 3A, 3B, 3C). There was a significant difference between the effects of 4-AP and TEA on the A-type current ($p < 0.05$, independent t test). The delayed rectifier-type current showed sensitivity similar to both drugs. Five mM 4-AP and 5 mM TEA reduced the delayed rectifier-type current recorded at the end of the 40 mV step pulse to $41.3 \pm 4.7\%$ and $52.7 \pm 3.2\%$ of the control (Fig. 3F, 3C), respectively. Those two values were not significantly different.

Hyperpolarization-activated inward current

With 147 mM NMGCl in the bath and 155 mM K^+ in the pipette, membrane hyperpolarization from 0 mV to -130 mV with -10 mV decrements elicited inward currents. Increasing the concentration of external K^+ from 5 mM to 30 or 60 mM made the slope of the current-voltage curve steeper and shifted the reversal potentials to positive values from -27.3 ± 3.8 mV to -20.3 ± 1.7 mV (30 mM $[\text{K}^+]_{\text{ext}}$) and -13.3 ± 0.9 mV (60 mM $[\text{K}^+]_{\text{ext}}$), respectively (Fig. 4A, 4B, 4C, 4D, $n=6$).

These inward currents were voltage-dependently blocked by cesium (Cs^+) or barium (Ba^{2+}). With 87 mM $[\text{NMG}^+]_{\text{ext}}$ and 60 mM $[\text{K}^+]_{\text{ext}}$, 3 μM Cs^+ suppressed the inward currents recorded at potentials negative to -90 mV, while the currents recorded at potentials positive to -90 mV were not significantly affected. The current recorded at -130 mV was reduced from -312.85 ± 91.8 pA to -70.71 ± 41.1 pA

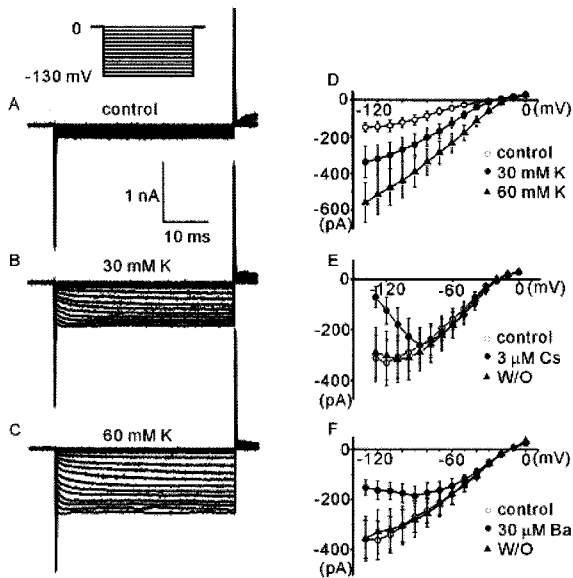


Fig. 4. Hyperpolarization-activated inward currents in hNSCs. (A~C) Hyperpolarizing pulses from 0 to -130 mV elicited inward currents, which exhibited increases in amplitude with increases in the external concentration of K^+ ($[K^+]_{ext}$). The I~V relationships of hyperpolarization-activated inward currents on external K^+ concentrations are shown in (D: hollow circle - control, filled circle -30 mM $[K^+]_{ext}$, filled triangle -60 mM $[K^+]_{ext}$). The cesium (Cs) or barium (Ba) reversibly blocked the hyperpolarization-activated inward currents (E, F: hollow circle - control, filled circle - Cs or Ba, filled triangle - wash out).

($n=7$, Fig. 4E) by $3 \mu M$ Cs^+ . External Ba^{2+} also showed similar inhibition. The current recorded at -130 mV was reduced from -358 ± 75.90 pA to -152.3 ± 30.7 pA by $30 \mu M$ Ba^{2+} ($n=7$, Fig. 4F).

DISCUSSION

Non-differentiating NSCs differ from differentiated neurons in many aspects including morphology, immunological markers and ionic channel expression patterns. Among them, the expression of inward currents (Na^+ , Ca^{2+} , K^+) has often been regarded as a marker for functionally active differentiated neurons (Piper et al, 2000; Cho et al, 2002). In particular, the presence of a Na^+ inward current might be a minimal and necessary condition for the functioning neuron in terms of generation of action potential. The Na^+ inward currents reported in this study resemble classical neuronal Na^+ currents in terms of their current-voltage relation, Na^+ -specificity and TTX-sensitivity. However, we did not observe any TTX-resistant Na^+ currents such as those in differentiated human neuronal precursor cells (cHNPCs) reported by Piper et al. (Piper et al, 2000). This TTX-resistant Na^+ current has rarely been reported in other NSC-derived neurons. Cho et al. reported Na^+ currents similar to those observed in this study in an immortalized hNSC line, HBL.F3, generated by the infection of human brain cell cultures with a retroviral vector containing *v-myc* (Cho et al, 2002). Although the HBL.F3 cell line originated from a human embryonic telencephalon tissue culture, the origin similar to our cells, the Na^+ current was observed only after the full-length coding region of NeuroD was

transfected into the HBL.F3 cells. Our result indicates that hNSCs derived from the same origin do not necessarily express similar ion channels. Piper et al. also observed Ca^{2+} inward currents, but they did not present the raw data. As Ca^{2+} channels are reported to play a key role in promoting neural stem/progenitor cell differentiation in mice (D'Ascenzo et al, 2006) and we observed a nicardipine-sensitive Ca^{2+} current in neuronal cells derived from human mesenchymal stem cells (unpublished observation), we expected to observe a Ca^{2+} current rather than a Na^+ current, when we initiated our experiments. However, we failed to observe an inward Ca^{2+} current. Ca^{2+} currents have been reported in many differentiated cells derived from different human stem cells (Li et al, 2005; Zahanich et al, 2005; Artiani et al, 2007), however they have rarely been observed in hNSCs. Some investigators have reported the expression of Ca^{2+} channels in hNSCs (Piper et al, 2000; Moe et al, 2005b). However, raw electrophysiological data have not been presented to date. A question of whether the absence of a Ca^{2+} channel in this study resulted from the innate characteristics of our cells or the culture conditions that we used will need to be clarified in future.

In the present study, we presented hyperpolarization-activated inward current. The amplitudes of the currents increased and the reversal potentials were altered by elevating the external K^+ concentration, demonstrating that the properties of these channels resemble those of inward rectifier K^+ currents. In particular, the voltage-dependent block by Ba^{2+} or Cs^+ is quite similar to those reported earlier (Flynn et al, 1999; Thompson et al, 2000; Murata et al, 2002), which indicated that this hyperpolarization-activated current was an inward rectifier K^+ -like current. However, the reversal potentials (-20.3 ± 1.7 mV at 30 mM $[K^+]_{ext}$, -13.3 ± 0.9 mV at 60 mM $[K^+]_{ext}$) did not match well with theoretical values (-42.2 mV at 30 mM $[K^+]_{ext}$, -24.4 mV at 60 mM $[K^+]_{ext}$), and the kinetics and voltage dependency did not resemble the properties of classical inward rectifier K^+ currents. Thus, this hyperpolarization-activated current may not reflect the activity of an inward rectifier K^+ channel. Other currents that may activate in these voltage ranges include the hyperpolarization-activated nonselective cation current and the HERG current. However, HERG channels would typically be closed at holding potentials negative to -80 mV, and the activation kinetics and Ba^{2+} sensitivity did not match well with the properties of hyperpolarization-activated nonselective cation currents. The family of inward rectifier K^+ channels is generally divided, on the basis of molecular and electrophysiological attributes, into seven subfamilies (Kir1.0~Kir7.0), which have more than 20 members (Doupnik et al, 1995; Nichols & Lopatin, 1997; Butt & Kalsi, 2006). We have not taken a molecular approach or a more detailed electrophysiological characterization of this hyperpolarization-activated inward current. Further investigation is needed to identify the channels involved.

The two types of outward K^+ currents presented in this study have also been reported in other hNSCs-derived neuronal cells (Piper et al, 2000; Westerlund et al, 2003; Moe et al, 2005b). In mesenchymal stem cells derived from human umbilical cord vein, another type of K^+ outward current, a Ca^{2+} -activated K^+ outward current, was observed (Park et al, 2007). When we recorded the K^+ outward currents in the present study, we used an internal solution containing a high concentration of Ca^{2+} buffer (10 mM EGTA). If the concentration of the Ca^{2+} buffer was lower,

it might be possible to record a Ca^{2+} -activated K^+ outward in these neuronal cells. In this study, we observed that 4-AP efficiently blocked the A-type K^+ current, however the effect of 4-AP was not limited only to this current. It also potently inhibited the delayed rectifier-type K^+ current. This lack of specificity of 4-AP has previously been reported in other systems. However, as 4-AP acts as a specific blocker of A-type currents in certain neuronal cells derived from human stem cells (Westerlund et al, 2003; Park et al, 2007), this non-specific inhibition by 4-AP should be regarded as one of the characteristics of these neuronal cells. The A-type current was not observed in the immortalized cell line, HBLF3, derived from a human embryonic telencephalon tissue culture (Cho et al, 2002), further supporting the observation that the same origin does not guarantee the same ionic channel expression pattern.

In this study, we characterized the expression pattern of ion channels in differentiated neural cells derived from hNSCs and compared some of our results with those of previous reports. However, as ion channel expression patterns could be altered by culture conditions, more detailed comparison with other cells is needed to elucidate the source of these differences.

REFERENCES

- Akesson E, Piao JH, Samuelsson EB, Holmberg L, Kjaeldgaard A, Falci S, Sundstrom E, Seiger A. Long-term culture and neuronal survival after intraspinal transplantation of human spinal cord-derived neurospheres. *Physiol Behav* 92: 60–66, 2007
- Artiani L, Bettiol E, Stillitano F, Mugelli A, Cerbai E, Jaconi ME. Developmental changes in cardiomyocytes differentiated from human embryonic stem cells: a molecular and electrophysiological approach. *Stem Cells* 25: 1136–1144, 2007
- Balasubramanian V, de Haas AH, Bakels R, Koper A, Boddeke HW, Copray JC. Functionally deficient neuronal differentiation of mouse embryonic neural stem cells in vitro. *Neurosci Res* 49: 261–265, 2004
- Butt AM, Kalsi A. Inwardly rectifying potassium channels (Kir) in central nervous system glia: a special role for Kir4.1 in glial functions. *J Cell Mol Med* 10: 33–44, 2006
- Buzańska L, Jurga M, Domańska-Janik K. Neuronal differentiation of human umbilical cord blood neural stem-like cell line. *Neurodegener Dis* 3: 19–26, 2006
- Carpenter MK, Inokuma MS, Denham J, Mujtaba T, Chiu CP, Rao MS. Enrichment of neurons and neural precursors from human embryonic stem cells. *Exp Neurol* 172: 383–397, 2001
- Cho T, Bae JH, Choi HB, Kim SS, McLarnon JG, Suh-Kim H, Kim SU, Min CK. Human neural stem cells: electrophysiological properties of voltage-gated ion channels. *Neuroreport* 13: 1447–1452, 2002
- D'Ascenzo M, Piacentini R, Casalbore P, Budoni M, Pallini R, Azzena GB, Grassi C. Role of L-type Ca^{2+} channels in neural stem/progenitor cell differentiation. *Eur J Neurosci* 23: 935–944, 2006
- Douppnik CA, Davidson N, Lester HA. The inward rectifier potassium channel family. *Curr Opin Neurobiol* 5: 268–277, 1995
- Flax JD, Aurora S, Yang C, Simonin C, Willis AM, Billingham LL, Jendoubi M, Sidman RL, Wolfe JH, Kim SU, Snyder EY. Engraftable human neural stem cells respond to developmental cues, replace neurons, and express foreign genes. *Nat Biotechnol* 16: 1033–1039, 1998
- Flynn ER, McManus CA, Bradley KK, Koh SD, Hegarty TM, Horowitz B, Sanders KM. Inward rectifier potassium conductance regulates membrane potential of canine colonic smooth muscle. *J Physiol* 518(Pt 1): 247–256, 1999
- Ilancheran S, Michalska A, Peh G, Wallace EM, Pera M, Manuelpillai U. Stem cells derived from human fetal membranes display multilineage differentiation potential. *Biol Reprod* 77: 577–588, 2007
- Johnson MA, Weick JP, Pearce RA, Zhang SC. Functional neural development from human embryonic stem cells: accelerated synaptic activity via astrocyte coculture. *J Neurosci* 27: 3069–3077, 2007
- Li GR, Sun H, Deng X, Lau CP. Characterization of ionic currents in human mesenchymal stem cells from bone marrow. *Stem Cells* 23: 371–382, 2005
- Mareschi K, Novara M, Rustichelli D, Ferrero I, Guido D, Carbone E, Medico E, Madon E, Vercelli A, Fagioli F. Neural differentiation of human mesenchymal stem cells: Evidence for expression of neural markers and eag K^+ channel types. *Exp Hematol* 34: 1563–1572, 2006
- Moe MC, Westerlund U, Varghese M, Berg-Johnsen J, Svensson M, Langmoen LA. Development of neuronal networks from single stem cells harvested from the adult human brain. *Neurosurgery* 56: 1182–1188, 2005a
- Moe MC, Varghese M, Danilov AI, Westerlund U, Ramm-Petersen J, Brundin L, Svensson M, Berg-Johnsen J, Langmoen IA. Multipotent progenitor cells from the adult human brain: neurophysiological differentiation to mature neurons. *Brain* 128: 2189–2199, 2005b
- Murata Y, Fujiwara Y, Kubo Y. Identification of a site involved in the block by extracellular Mg^{2+} and Ba^{2+} as well as permeation of K^{+} in the Kir2.1 K^{+} channel. *J Physiol* 544: 665–677, 2002
- Nichols CG, Lopatin AN. Inward rectifier potassium channels. *Ann Rev Physiol* 47: 11–39, 1997
- Park KS, Jung KH, Kim SH, Kim KS, Choi MR, Kim Y, Chai YG. Functional expression of ion channels in mesenchymal stem cells derived from umbilical cord vein. *Stem Cells* 25: 2044–2052, 2007
- Piper DR, Mujtaba T, Rao MS, Lucero MT. Immunocytochemical and physiological characterization of a population of cultured human neural precursors. *J Neurophysiol* 84: 534–548, 2000
- Sun W, Buzanska L, Domanska-Janik K, Salvi RJ, Stachowiak MK. Voltage-sensitive and ligand-gated channels in differentiating neural stem-like cells derived from the nonhematopoietic fraction of human umbilical cord blood. *Stem Cells* 23: 931–945, 2005
- Thompson GA, Leyland ML, Ashmole I, Sutcliffe MJ, Stanfield PR. Residues beyond the selectivity filter of the K^{+} channel kir2.1 regulate permeation and block by external Rb^{+} and Cs^{+} . *J Physiol* 526: 231–240, 2000
- Weiss S, Reynolds BA, Vescovi AL, Morshead C, Craig CG, Van der Kooy D. Is there a neural stem cell in the mammalian forebrain? *Trends Neurosci* 19: 387–393, 1996
- Westerlund U, Moe MC, Varghese MM, Berg-Johnsen J, Ohlsson M, Langmoen IA, Svensson M. Stem cells from the adult human brain develop into functional neurons in culture. *Exp Cell Res* 289: 378–383, 2003
- Zaharich I, Graf EM, Heubach JF, Hempel U, Boxberger S, Ravens U. Molecular and functional expression of voltage-operated calcium channels during osteogenic differentiation of human mesenchymal stem cells. *J Bone Miner Res* 20: 1637–1646, 2005